Semi-empirical methods for evaluating liquefaction risk using PMT-SPT correlations and finite element modeling

Évaluation du risque de liquéfaction par approches semi-empiriques basées sur les corrélations PMT-SPT et la modélisation par éléments finis

Fatima Ezzahraa LATIFI[1#] and *Khadija* BABA[2]

[1]*Civil Engineering, Water, Environment and Geosciences Centre, Mohammadia School of Engineering*
Mohammed V University, Rabat, Morocco
[2]*Civil Engineering and Environment Laboratory, Hight School of Technology, Sale*
Mohammed V University, Rabat, Morocco
[1#]*Fatima Ezzahraa LATIFI: fatimaezzahraa_latifi@um5.ac.ma*
[2]*Khadija BABA : khadija.baba@est.um5.ac.ma*

ABSTRACT

Since the 1964 Niigata and Alaska earthquakes, soil liquefaction has become a critical concern in geotechnical engineering. This study investigates the liquefaction susceptibility of a site 3 km south of Tétouan, in the Western Rif region of northern Morocco, known for its seismic activity per RPS 2011. The analysis uses a combination of semi-empirical methods and numerical modeling, correlating Ménard Pressuremeter Test (PMT) and Standard Penetration Test (SPT) results. Liquefaction potential (LP) is evaluated using cyclic stress-based approaches from Youd et al. (2001) and Idriss et al. (2004), supported by simulations using the UBC3D-PLM model. Findings reveal high liquefaction susceptibility in sandy marl layers at 4–5 m and 15.5–17.5 m depths, with LP values ranging from 0.65 to 0.85, indicating strong likelihood. Slightly gravelly sand layers between 5 and 12 m show LP > 0.85, suggesting near-certain liquefaction. Conversely, greyish sandy marl (2–4 m and 17.5–19.5 m) and greyish slightly gravelly sand (12–15.5 m) display moderate LP values between 0.35 and 0.65, reflecting uncertain liquefaction potential. Layers deeper than 19.5 m show very low susceptibility (PL < 0.15).Overall, semi-empirical and numerical results align closely, though some intermediate layers present uncertainty. The study highlights the Ménard pressuremeter test as a valuable and dependable tool for assessing liquefaction risk, especially through boundary pressure correlations. Its integration is highly recommended in geotechnical evaluations for construction and land development in seismically active zones.

Keywords: Liquefaction potential; Menard pressuremeter test (PMT); Standard penetrometer test (SPT); Semi-Empirical Methods.

RESUME

Depuis les séismes de Niigata et d'Alaska en 1964, la liquéfaction des sols constitue une problématique majeure en ingénierie géotechnique. La présente étude évalue la susceptibilité à la liquéfaction d'un site localisé à 3 km au sud de Tétouan, dans le Rif occidental (nord du Maroc), une zone sismiquement active selon le RPS 2011. L'approche adoptée combine des méthodes semi-empiriques basées sur la contrainte cyclique avec une modélisation numérique via le modèle UBC3D-PLM, en s'appuyant sur la corrélation entre les résultats des essais pressiométriques Ménard (PMT) et ceux des essais de pénétration standard (SPT).Les résultats issus des méthodes de Youd et al. (2001) et Idriss et al. (2004) révèlent une forte susceptibilité à la liquéfaction pour les couches de marne sableuse situées entre 4–5 m et 15,5–17,5 m, avec un potentiel de liquéfaction (PL) compris entre 0,65 et 0,85. Les couches de sable légèrement graveleux entre 5 et 12 m présentent un PL > 0,85, indiquant une liquéfaction quasi certaine. En revanche, les horizons de marne sableuse grisâtre (2–4 m, 17,5–19,5 m) et de sable légèrement graveleux grisâtre (12–15,5 m) présentent un PL compris entre 0,35 et 0,65, traduisant une probabilité incertaine. Les couches situées au-delà de 19,5 m montrent une très faible susceptibilité (PL < 0,15).
Les résultats semi-empiriques s'accordent globalement avec ceux de la modélisation numérique. L'étude confirme la fiabilité du PMT comme outil pertinent d'évaluation du risque de liquéfaction, dont l'intégration est vivement recommandée pour les projets en zones à fort aléa sismique.

Keywords : Potentiel de liquéfaction ; essai pressiométrique de Ménard (PMT) ; essai pénétrométrique standard (SPT) ; méthodes semi-empiriques.

1. Introduction

Liquefaction is a phenomenon in which soil in a saturated area loses a significant portion of its shear strength and reacts like a fluid under the effect of monotonic or cyclic shear loads expressed by Castro et Poulos (1977) [6-18]. For a soil in saturated state, the dissipation of pore water pressure can be hindered by the presence of clay or silt inclusions or by a rapid load application that does not allow sufficient time for drainage. Under such conditions, the soil's tendency to compact leads to an augmentation in pore water pressure, a decrease in effective stress, and, consequently, the progressive loss of shear strength.

When surplus pore water pressure approaches the first vertical effective stress of a purely frictional soil, shear resistance is entirely lost at that location, causing the soil to liquefy with behavior such as a viscous fluid.

Since the 1964 seisms in Niigata and Alaska [21- 22-30-34-41-42], scientific interest in soil liquefaction has continued to grow due to the significant human and economic losses it causes. A recent example is the September 28, 2018, earthquake in Indonesia [43], where liquefaction resulted in more casualties than the earthquake itself or the subsequent tsunami. In response to these risks, numerous research projects have been conducted to introduce semi-empirical methods to assess the risk of liquefaction.

This phenomenon primarily Influenced by the intrinsic of soil's characteristics, such as its relative density, granulometry, texture, saturation, and the magnitude of applied seismic loads. Initially assessed through laboratory testing, liquefaction studies now rely on in-situ tests as well as the cone penetration test (CPT) [48] and the standard penetration test. Accuracy of liquefaction assessments strongly depends on the quality of site characterization, which must be conducted in accordance with current standards. Three main methodological approaches exist: the strain-based approach [19-29], the energy-based approach [31], and the stress-based approach [35-39-40].

In this study, we focused on the widely used and advanced strain-based approach, which establishes a correlation between cyclic strain and cyclic resistance, crucial for understanding liquefaction behavior. Our study is organized into two elements: the first provides detailed assessment of liquefaction potential in a region located in northern Morocco. To achieve this, we analyze geographic, geological, and seismic parameters and apply two semi-empirical methods, those of Idriss et al. (2004) [39] and Youd et al. (2001)[15] , based on the correlation established by H. Gonin et al. (1992)[14] between the (PMT) [6] and the (SPT) [17].

For the second part, we integrate the UBC3D-PLM [32-7-11-8] constitutive model into Plaxis 2D , requiring precise calibration using laboratory and field test data. This approach aims to enhance our understanding of liquefaction potential in the studied area and validate the results of the semi-empirical methods through numerical modeling.

2. Prediction of soil liquefaction using semi-empirical methods

2.1. Evaluating liquefaction probability

Nowadays, the vulnerability of soil to liquefaction, assessed through the liquefaction potential (PL), can be estimated using various semi-empirical methods. In other words, this parameter represents the ability for soil to resist seismic forces and is heavily influenced by factors such as soil composition, groundwater table depth, grain size distribution, relative density, and earthquake magnitude [1-2-3].

Insights gained from in-situ testing and the analysis of past seismic events have contributed to the development of semi-empirical approaches. These methodologies are generally categorized into three major classes: the cyclic deformation method, the energetic method, and the cyclic stress method.

Furthermore, laboratory investigations have been conducted to evaluate liquefaction susceptibility by analyzing soil behavior under earthquake conditions [12-13]. In this context, in-situ testing remains a widely used approach for assessing liquefaction hazards. Specifically, undisturbed soil samples can be retrieved using the cone penetration test [45-46] and the standard penetration test.

This study focuses on the cyclic stress method to examine soil response to seismic activity. More precisely, we will calculate the safety factor (Fs), which represents the proportion between the cyclic stress rate (CSR) and the cyclic resistance rate (CRR) [25-24-39-40], utilizing data obtained from correlations between the Ménard pressuremeter test and the Standard Penetration Test .

The liquefaction probability PL is determined based on the safety factor value and is computed using the following simplified equation (Equation 1):

$$P_L = \frac{1}{1+\left(\frac{F_S}{A}\right)^B} \quad (1)$$

Where:

- A= 0,96 ; B= 4,50 according Juang method [20]
- A= 1 ; B=2,78 according Olsen method [31]
- A=1 ; B= 3,30 according Robertson and Wride method [35]

Based on the liquefaction likelihood index given by formula 1, the liquefaction order and its instance can be determined and interpreted using Table 1.

Table 1. Occurrence of liquefaction according to the liquefaction probability index [7-11]

Liquefaction probability index	Class	Liquefaction probability
$P_L \geq 0,85$	5	Liquefaction almost certain
$0,65 \leq P_L < 0,85$	4	Liquefaction highly probable
$0,35 \leq P_L < 0,65$	3	Non-liquefaction and liquefaction are feasible
$0,15 \leq P_L < 0,35$	2	Liquefaction unlikely to occur
$P_L < 0,15$	1	Non-liquefaction almost certain

In this article, the proposed assessment methods [37-23-25] are developed using the cyclic stress approach, utilizing the correlation between Menard penetrometer test and the SPT test. This demands the calculation of the cyclic stress rate (CSR) and the cyclic resistance rate (CRR), to assess the (Fs), which is shown by formula (2).

$$F_S = \frac{CRR}{CSR} \quad (2)$$

2.2. Evaluating the safety factor

2.3. Calculating Cyclic Stress Ratio (CSR)

The (CSR) quantifies a relationship between the cyclic shear stress within a soil layer (τ_{avg}) [46-26] and the effective vertical stress (σ'_v)[44-45]. This parameter is crucial in evaluating soil vulnerability to liquefaction under seismic loading conditions.

Originally formulated by Seed and Idriss in 1971 [39], the CSR is expressed mathematically in equation (3) as follows:

$$\mathrm{CSR} = \frac{\tau_{av}}{\sigma'_v} = 0,65 \left(\frac{a_{max}}{g}\right)\left(\frac{\tau_{av}}{\sigma'_v}\right) r_d \quad (3)$$

The parameter (a_{max}) denotes the peak horizontal acceleration induced by seismic activity, while G=9.81 m/s² represents the standard gravitational acceleration. Effective vertical stress (σ'_v) corresponds to total stress exerted by the overlying soil layers. (r_d) is the stress reduction factor, which accounts for the mitigation of shear stress with increasing depth caused by the soil's dynamic response and flexibility.

A coefficient of (0.65) is applied to transform the maximum (CRR) into an equivalent (CSR), reflecting the dominant loading cycles throughout the earthquake duration. This adjustment enhances the accuracy of liquefaction susceptibility assessments by considering the most representative stress cycles rather than peak values alone.

The stress reduction factor (r_d) is depth-dependent and is determined using the following equations (4), as formulated by Liao and Whitman (1986) [26]:

$$rd = 1 - 0,00765 \quad \text{if we have : } z \leq 9,15\ m \quad (24)$$

$$rd = 1 - 0,00765\ z \quad \text{if we have : } 9,15\ m < z \leq 23\ m \quad (4)$$

In the methodology introduced by Idriss [15] for assessing liquefaction potential, Equation (3) has been revised to integrate two supplementary parameters. These modifications enhance the initial model, improving its precision in forecasting soil response to seismic forces. By incorporating these additional factors, the updated equation provides a more realistic representation of field conditions, thereby increasing the reliability of liquefaction evaluations. The refined mathematical expression is as follows:

$$\mathrm{CSR} = \frac{\tau_{av}}{\sigma'_v} = 0,65 \left(\frac{a_{max}}{g}\right)\left(\frac{\tau_{av}}{\sigma'_v}\right) \frac{r_d}{\mathrm{MSF}} \frac{1}{K_\sigma} \quad (5)$$

Where:

The MSF factor, according to the method proposed by Idriss in 1999 [16], is given by the following formula (6):

$$\mathrm{MSF} = 6,9exp\left(\frac{-\mathrm{M}}{4}\right) - 0.058 \quad (6)$$

The vertical effective stress correction factor, denoted as (K_σ), is defined by Boulanger and Idriss [9] in equation (7) as follows:

$$K_\sigma = 1 - C_\sigma ln\left(\frac{\sigma_{v0}}{P_a}\right) \quad (7)$$

2.4. Calculating Cyclic Resistance Ratio (CRR)

2.5. Youd et al.(2001) method

The approach established by Youd et al. (2001) [48] stems from a workshop held in 1996, corporated by the National Center for Earthquake Engineering Research (NCEER)[19]. This event brought together 20 experts to evaluate advancements in liquefaction potential assessment methods over the preceding decade [11]. The (CRR) is calculated using the equation 8:

$$\mathrm{CRR} = \frac{1}{34 - \mathrm{N}_{1,60}} + \frac{\mathrm{N}_{1,60}}{35} + \frac{50}{(10\mathrm{N}_{1,60}+45)^2} - \frac{1}{200} \quad (8)$$

2.6. Idriss et al. (2004) Method

The methodology proposed by Idriss and Boulanger (2004) [39] reexamines correlations in the assessment of liquefaction potential. They advocate for the application of the following equation to compute the (CRR) for a magnitude 7.5 seism, considering an effective vertical stress $\sigma'_v = 1atm$ as a function of $\mathrm{N}_{1,60}$.

$$\mathrm{CRR} = \exp\left\{\frac{\mathrm{N}_{1,60}}{14,1} + \left[\frac{\mathrm{N}_{1,60}}{126}\right]^2 - \left[\frac{\mathrm{N}_{1,60}}{23,6}\right]^3 + \left[\frac{\mathrm{N}_{1,60}}{25,4}\right]^4 - 2,8\right\} \quad (9)$$

2.7. Correlation methods between (PMT) the Ménard Pressuremeter Test and (SPT) the Standard Penetration Test.

Correlation method proposed by Honin et al. (1992) [14] relies on matching the results of the (SPT) and (PMT) tests across various geological formations. The goal is to identify relationships between the number of blows required to drive (SPT) the Standard Penetration Test

sampler and the limiting pressures obtained from (PMT) the Menard Pressuremeter Test. The study developed correlations for five primary soil types in which both SPT and pressuremeter tests are applied, as summarized in Table 2.

Table 2: Correlation proposed between N (SPT) and P_L (PMT)

Soil nature	$P_L \rightarrow N$
Silt	N= 32 x P_L
Sands	N= 21 x P_L
Greeb clays	N= 26 x P_L
Plastic clays	N= 18 x P_L
Marl	N= 23 x P_L
Chalk	N= 6 x P_L

The number of blows recorded in the (SPT) Standard Penetration Test, used like an indicator of soil liquefaction characteristics, requires distinguishing the influence of the density of the soil and effective vertical stress on the resistance to penetration. As a result, Seed et al [39-4-5] incorporated the standardization of sand resistance to penetration to a factor equivalent to atmospheric pressure into the semi-empirical process. This strandarization is now represented as follows:

$$N_{1,60} = C_N \, x \, N_1 \quad (10)$$

In this study, following the approach of Idriss and Boulanger [19], we used equation (11) to calculate the C_N value, which is given by the following expression:

$$C_N = \left(\frac{P_a}{\sigma'_{v0}}\right)^{\alpha} \quad (11)$$

where:

$$\alpha = 0{,}784 - 0{,}0768\sqrt{N_1} \quad (12)$$

3. Liquefaction Prediction UsingUBC3D-PLM Model in Plaxis 2D

The UBC3D-PLM model, initially developed by Puebla et al. (1997) [28 -20-8] later refined by Tsegaye (2010)[47] for PLAXIS integration. Further improvements by Galavi and Petalas (2013)[33] enhanced its performance, particularly under monotonic loading.

Rooted in classical plasticity theory, it incorporates a hyperbolic strain-hardening rule and applies a Mohr-Coulomb failure criterion with a modified plastic potential function based on the Drucker-Prager[10] criterion.

Designed to model excess pore water pressure and soil liquefaction under dynamic loading, the model follows an elastoplastic framework, distinguishing between elastic and plastic deformations. Its nonlinear elastic behavior is governed by the shear modulus (G) and bulk modulus (K), both considered isotropic, with their stress dependency expressed as follows:

$$K = K_B^e P_A \left(\frac{p}{P_{ref}}\right)^{me} \quad (13)$$

$$G = K_G^e P_A \left(\frac{p}{P_{ref}}\right)^{ne} \quad (14)$$

Where:

- K_G^e is the elastic shear modulus,
- K_B^e is the elastic bulk modulus,
- P_{ref} is reference stress level, taken as atmospheric pressure P_A =100kPa
- *ne* and *me* define the stiffness reliance level on stress.

Like most liquefaction models, the input of the UBC3D-PLM constitutive model are generally obtained through curve fitting, ideally using undrained cyclic direct shear tests. However, such tests are not always accessible, leading researchers to rely on in-situ investigations, such as cone (CPT) or (SPT) tests, as viable alternatives. In response to this limitation, Beaty and Byrne (2001) established a series of correlations that relate the number of SPT equivalent shots $(N_1)_{60}$ [8] to the model parameters, as outlined in Table 3. These correlations are defined as follows:

Table 3. UBC3D-PLM parameters

PARAMETER	DESCRIPTION
K_G^e	Elastic Shear Modulus
K_B^e	Elastic Bulk Modulus
K_G^p	Plastic Shear Modulus
$(N_1)_{60}$	Corrected SPT value
φ_{cv}	Constant volume friction angle
φ_p	Peak friction angle
R_f	Failure Ratio
fac_{hard}	Densification Factor
fac_{post}	Post Liquefaction Factor
P_A	Atmospheric pressure
NE	Elastic Shear Modulus Index
ME	Elastic Bulk Modulus Index

4. Case study

4.1. Geographical location

The zone of study is located in northern Morocco, about 3 km from Tetouan towards Chefchaouen. The project entails constructing the Tamuda Bridge over the Martil River, situated along the expressway connecting Tetouan and Chefchaouen. Illustration 1 presents a satellite view of the site, which can be accurately identified using the Lambert coordinates:
X = 498,725; Y = 551,008

Figure 1. Satellite view of the study area

4.2. Geological Context

The zone of study, located in the western Rif, shows a diverse range of geological formations. It includes Jurassic sedimentary sequences, primarily composed of limestone, alongside more recent deposits of clay and marl, reflecting environmental variations across different geological periods.

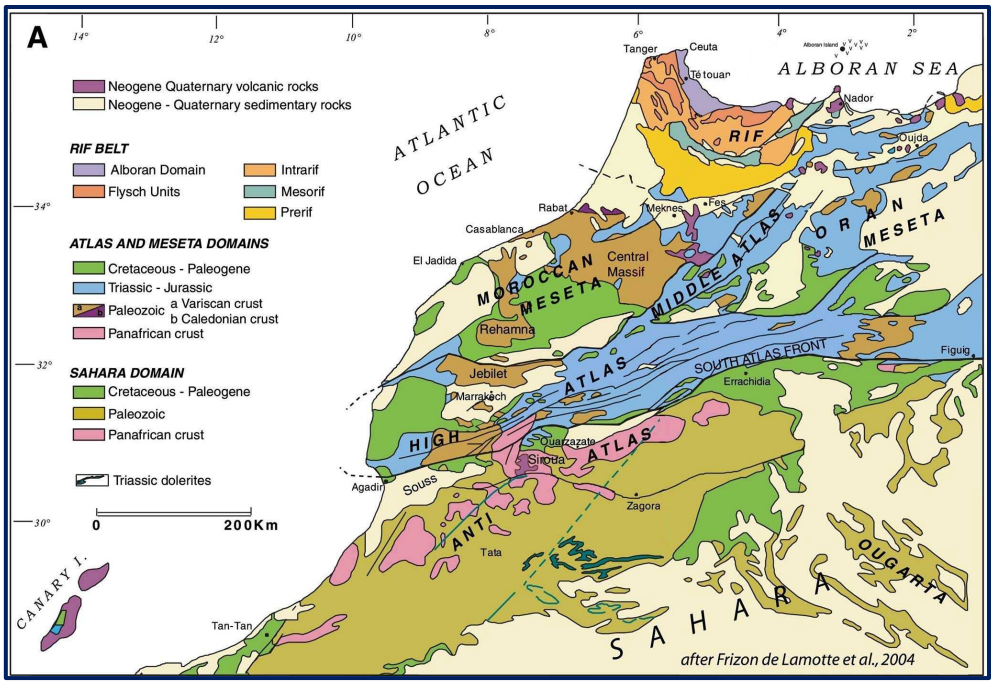

Figure2. Geography of the Study Area [27]

4.3. Context and Geotechnical Reconnaissance

The lithology of the study area exhibits significant variation with depth. The identified formations are as follows:

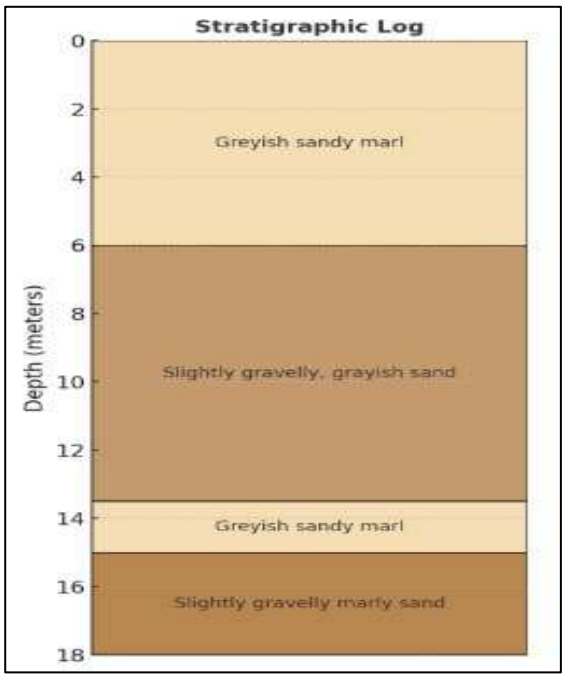

Figure3. Stratigraphic Log of the Study Area

- The uppermost six meters consist of a greyish sandy marl layer,
- Between 6 and 13.5 meters, a layer of slightly gravelly, grayish sand is present.
- From 15 to 16.5 meters, the greyish sandy marl layer reappears,
- At deeper levels, extending to 19.5 meters, a layer of slightly gravelly marly sand is encountered.

4.4. Seismicity in the Study Area

Morocco is systematically divided into five distinct seismic zones, ranging from Zone 0, which has an extremely low seismic risk, to Zone 4, where the risk is significantly high. This classification, established by the Moroccan Seismic Regulations (RPS 2011)[37], is determined based on key parameters such as ground acceleration and site characteristics and is meticulously mapped at the national level. The country's seismic zoning map visually illustrates the distribution of seismic risk across these zones, expressed in terms of maximum ground acceleration and velocity. Following RPS 2011 guidelines, the seismic parameters considered for the classification of the analyzed zone include:

- Seismic area classified in speed zone N°3, with speed v= 13 cm/s (Figure 4).

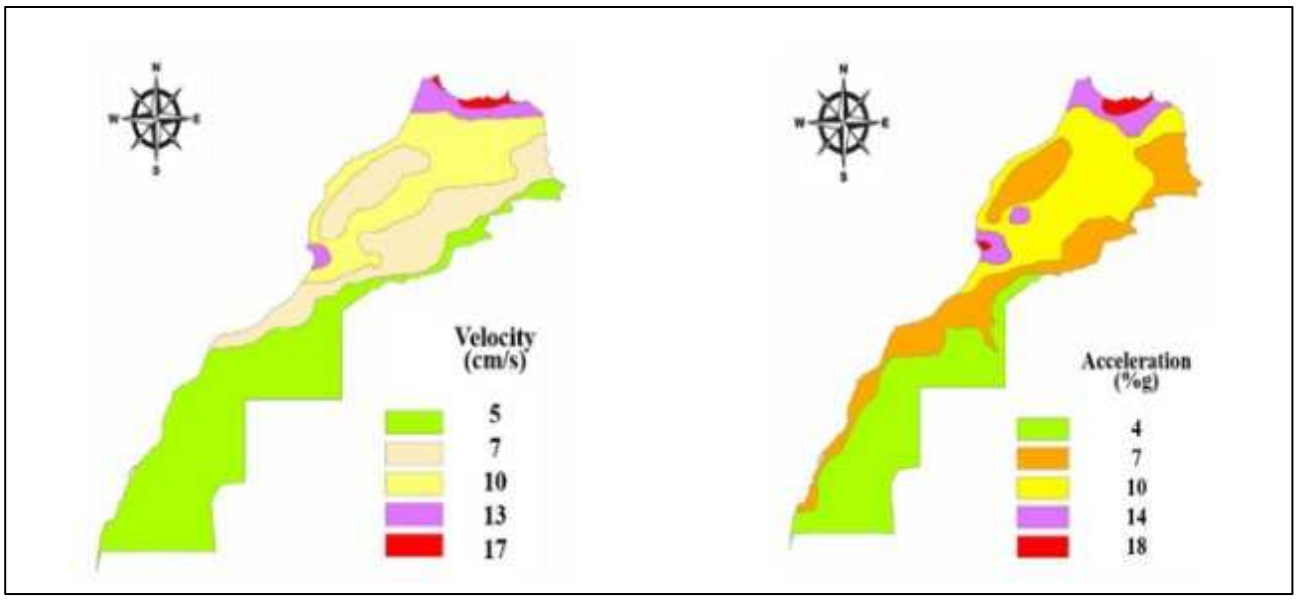

Figure 4. Zoning for seismic acceleration and velocity at 10% probability level over 50- Year period [37]

4.5. Results and Discussions

4.5.1. Results of correlation in Semi-empirical Methods

Considering the semi-empirical methods by Youd et al. (2001)[47] and Idriss et al. (2004)[38], which are based on the cyclic approach, as well as the correlation between the Ménard Pressumeter test (PMT) the Standard Penetration Test (SPT), Table 4 provides the CSR, CRR, FS, and PL values for different depths of soil layers.

Table 4. Semi-empirical methods results.

Depth (m)	Soil Nature	Youd et al. (2001)				Idriss et al.(2004)			
		CRR	CSR	Safty factor (Fs)	PL Index	CRR	CSR	Safty Factor (Fs)	PL Index
1,5	Greyish sandy marl	0,27	0,25	1,05	0,40	0,10	0,09	1,15	0,31
3		0,33	0,36	0,91	0,55	0,12	0,13	0,92	0,54
6	Slightly gravelly, grayish sand	0,15	0,45	0,33	0,99	0,08	0,16	0,49	0,95
7,5		0,19	0,48	0,39	0,98	0,09	0,17	0,51	0,94
9		0,32	0,50	0,65	0,86	0,12	0,18	0,66	0,85
10,5		0,31	0,51	0,62	0,88	0,12	0,18	0,63	0,87
12		0,43	0,52	0,82	0,68	0,14	0,19	0,76	0,74
13,5		0,54	0,53	1,02	0,43	0,17	0,19	0,91	0,56
15	Greyish sandy marl	0,53	0,54	0,98	0,48	0,17	0,19	0,88	0,60
16,5		0,31	0,54	0,58	0,91	0,12	0,20	0,59	0,90
18	Slightly gravelly marly sand	0,57	0,55	1,04	0,41	0,18	0,20	0,93	0,54
19,5		0,78	0,55	1,41	0,15	0,27	0,20	1,35	0,18

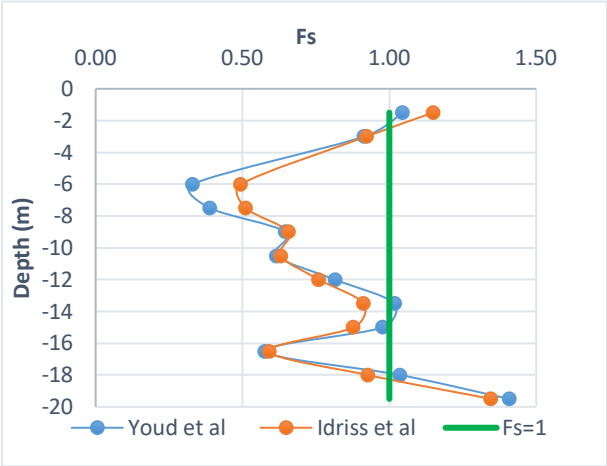

Figure 5. FS variation of the study area

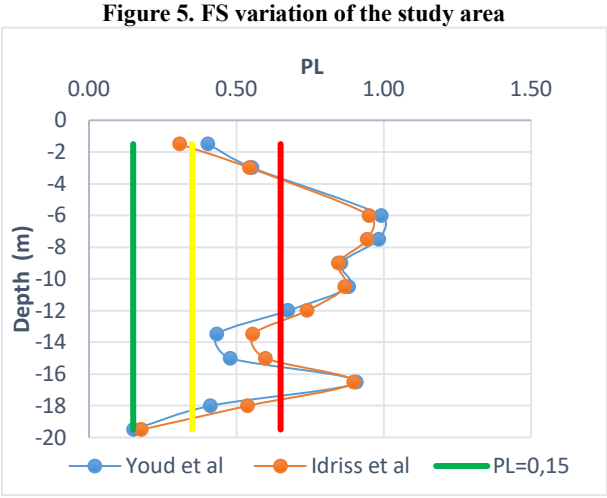

Figure6. PL variation of the study area

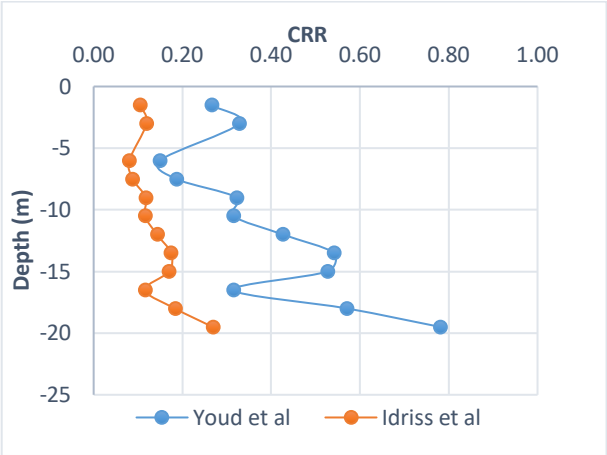

Figure 8. CRR variation of the study area

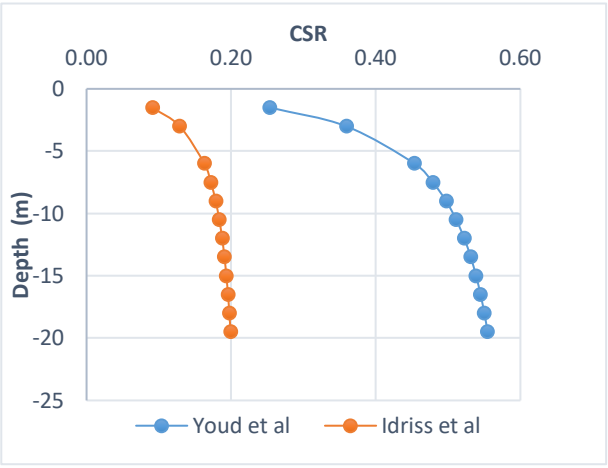

Figure 7. CSR variation of the study area

In Figure 5, we can confirm that certain points have a safety factor (Fs) below 1, indicating their vulnerability to liquefaction. Additionally, the change in the Fs charts for both methods is nearly identical in the study area. This

similarity is primarily attributed to the changes observed in the CSR curves in Figure 7 and the CRR curves in Figure 8.

Upon analyzing the various graphical representations of liquefaction potential from the methods shown in Figure 6, the conclusions can be reached is as follows :

- Soil layers between 6 and 12 meters deep, consisting of slightly gravelly sands, exhibit a high susceptibility to liquefaction, with a liquefaction potential (LP) ranging from 0.65 to 0.85 for both methods. Likewise, at a depth of 16.5 meters, layers made of sandy marl also demonstrate a significant liquefaction risk.
- There is a mixed probability of liquefaction and non-liquefaction for soil layers located between 3 and 4 meters deep, as well as between 17 and 18 meters, which are made up of sandy marl. The same behavior is noted for layers between 12 and 15.5 meters and between 18 and 19.5 meters, composed of slightly gravelly sand.
- Liquefaction is highly improbable in soil layers deeper than 19.5 meters, where the liquefaction potential (LP) is below 0.15.

4.5.2. Constitutive UBC3D-PLM Model Results on 2DPlaxis

4.5.2.1. UBC3D-PLM Model calibration

On the basis of the 2011 Moroccan RPS Guide [37], the study area falls within velocity and acceleration Zone No. 3. To assess its liquefaction potential using Plaxis 2D, input parameters of the UBC3D-PLM model were calibrated, as listed in Table 5 above:

Table 5. Model calibration

Parameter	Symbol	Unit	Layer1	Layer2	Layer3	Layer4
Elastic Shear Modulus	K_G^e	-	904,09	930,24	1022,21	1195,59
Elastic Bulk Modulus	K_B^e	-	632,87	651,17	715,55	836,91
Plastic shear modulus	K_G^p	-	322,63	371,86	626,27	1677,25
Corrected SPT value	$(N_1)_{60}$	-	9,06	9,87	13,10	20,97
Constant volume friction angle	φ_{cv}	(°)	27,20	27,20	27,20	27,20
Maximum angle of friction	φ_p	(°)	29,01	29,17	29,82	31,39
Faillure ratio	R_f	-	0,79	0,78	0,75	0,70
Densification factor	fac_{hard}	-	1,00	1,00	1,00	1,00
Atmospheric pressure	P_A	kPa	100,00	100,00	100,00	100,00
Elastic shear modulus index	ne	-	0,50	0,50	0,50	0,50
Elastic bulk modulus index	me	-	0,50	0,50	0,50	0,50
Dimension less factor, considers the non-linear relation between rigidity and plastic shear modulus	np	-	0,40	0,40	0,40	0,40

4.5.2.2. UBC3D-PLM Model Output on Plaxis 2D

The active pore pressure values after a seismic event are determined in figure 9. where we can see a marked increase in those layers susceptible to liquefaction under seismic solicitations.

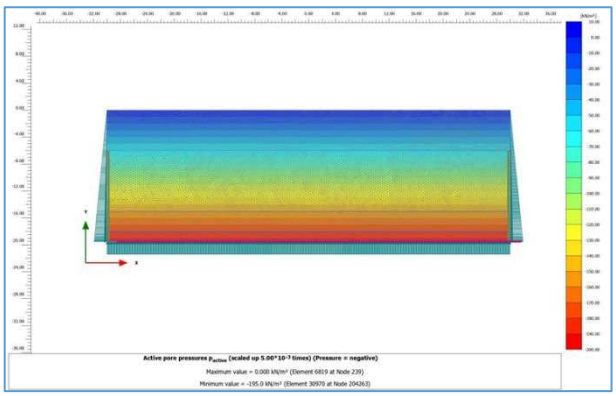

Figure 9: Active pore pressures

Effective stress levels following an earthquake are depicted in Figure 10, which shows a notable

rise in layers that could liquefy in reaction to seismic shaking.

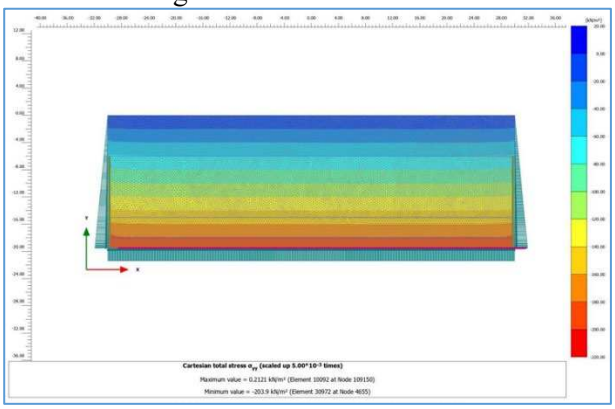

Figure 10: Cartesian total stress

Figure 11 presents a comprehensive analysis of liquefaction points using Plaxis 2D, emphasizing the precision of predictability using the UBC3D-PLM elastoplastic model in evaluating liquefaction potential in soil layers. The simulation reveals significant vulnerability to liquefaction across various soil layers, particularly the slightly gravelly sands, greyish sandy marls, and brown to greyish slightly gravelly marly sands.

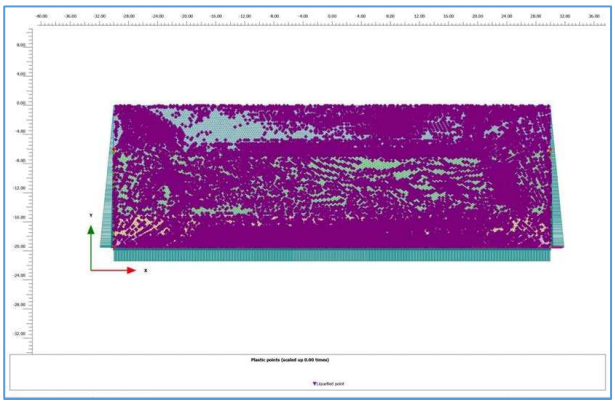

Figure 11: Liquified point

4.6. Summary and comparison

Overall, examination of the various graphical representations of the results of the semi-empirical methods employed (Youd et al.(2001) and Idriss et al.(2004) and numerical simulations using the UBC3D-PLM constitutive model on Plaxis 2D leads to the following conclusions:

- According to the two approaches examined, soil layers with slightly gravelly sand that are 5–12 meters below the surface have a liquefaction potential (LP) greater than 0.85, which indicates an almost certain risk of liquefaction.
- The horizons located between 4 and 5 meters and between 15.5 and 17.5 meters, made up of sandy marl, also show a high probability of liquefaction, with PL values between 0.65 and 0.85 according to the two semi-empirical approaches, results corroborated by numerical modeling.
- Significant uncertainty remains for layers between 2 and 4 meters, and between 17.5 and 19.5 meters (sandy marl), as well as for those between 12 and 15.5 meters and between 18 and 19.5 meters (slightly gravelly sand), where semi-empirical methods indicate an intermediate probability of liquefaction. However, numerical modelling suggests a higher susceptibility to liquefaction in all these layers.
- Finally, although semi-empirical methods indicate a very low probability of liquefaction for soils above 19 meters (PL < 0.15), numerical simulation results reveal a certain susceptibility to liquefaction even at these depths.

5. Conclusions

Our study provides a comprehensive analysis that enhances our understanding of soil behavior under seismic hazards. The results obtained from semi-empirical methods were validated through numerical modeling using the same input data, primarily based on the correlation between (PMT) the pressuremeter test [6] and (SPT) the standard penetration test [48].

The study area demonstrates a high susceptibility to liquefaction, particularly in soil layers between 6 and 12 meters deep, composed of slightly gravelly sands. Similarly, at a depth of 16.5 meters, sandy marl layers also exhibit a significant liquefaction potential, as indicated by both semi-empirical methods. Additionally, the Plaxis 2D simulation, utilizing the UBC3D-PL constitutive model, confirms that the various soil layers in this zone are highly likely to liquefy under seismic loading.

References

[1] Ahatri, M., and Baba, K. "The seismic motion parameters effects on response spectra: Comparison between El Centro 1940 and Imperial Valley 1979 earthquakes"

[2] Ahatri, M., Baba, K., Touijrate, S., and Bahi, L. 2018. "Characteristics of spectral responses for a ground motion from Mediterranean earthquake – Zeghanghane station (6.3Mw) in Morocco, and its influence on the structures", MATEC Web Conf, 149,02041.http://doi.org/10.1051/matecconf/201814902041.

[3] Ahatri, M., Baba, K., Touijrate, S., and Bahi, L. 2019. "The influence of spectral responses on the structures heights", In: Rodrigues, H., and Elnashai,

A., eds. Advances and Challenges in Structural Engineering, in Sustainable Civil Infrastructures. Cham: Springer International Publishing, pp. 65–76. http://doi.org/10.1007/978-3-030-01932-7_7.

[4] Ardouz, G., Baba, K., El Bouanani, L., Latifi, F. E., and Dardouch, A. 2022. "The influence of the fundamental parameters on the mechanical behavior of coarse-grained soils", Civil Eng J, 8(8), pp. 1694–1711.http://doi.org/10.28991/cej-2022-08-08-012.

[5] Ardouz, G., Baba, K., El Bouanani, L., Latifi, F. E., and Dardouch, A. 2022. "Novel methodology for determining the mechanical characteristics of coarse-grained soils", Civil Environ Eng, 18(2), pp. 540–550. http://doi.org/10.2478/cee-2022-0052.

[6] Bouafia, A. 2011. Les essais in-situ dans les projets de fondations, Office des publications universitaires, Place centrale de Ben-Aknoun, Alger, Algérie.

[7] Beaty, M., and Byrne, P. 1998. "An effective stress model for predicting liquefaction behavior of sand", In: Geotechnical Earthquake Engineering and Soil Dynamics III, ASCE Geotechnical Special Publication No. 75(1), pp. 766–777.

[8] Beaty, M., and Byrne, P. 2011. "UBCSAND constitutive model: Version 904aR", Journal of Geotechnical and Geoenvironmental Engineering, 137(8),pp.770–773. http://doi.org/10.1061/(ASCE)GT.1943-5606.0000513.

[9] Boulanger, R. W., and Idriss, I. M. 2004. "State normalization of penetration resistance and the effect of overburden stress on liquefaction resistance", In: Proc. 11th International Conference on Soil Dynamics and Earthquake Engineering and 3rd International Conference on Earthquake Geotechnical Engineering, University of California, Berkeley, CA.

[10] Drucker, D. C., and Prager, W. 1952. "Soil mechanics and plastic analysis for limit design", Q Appl Math, 10(2), pp. 157–165.

[11] El Bouanani, L., Baba, K., Ardouz, G., and Latifi, F. E. 2022. "Parametric study of a soil erosion control technique: concrete lozenges channels", Civil Eng J, 8(9), pp. 1879–1889. http://doi.org/10.28991/cej-2022-08-09-09.

[12] El Majid, A., Baba, K., and Razzouk, Y. 2023. "Assessing the impact of plant fibers on swelling parameters of two varieties of expansive soil", Case Stud Chem Environ Eng, 8, 100408. http://doi.org/10.1016/j.cscee.2023.100408.

[13] El Majid, A., Cherradi, C., Baba, K., and Razzouk, Y. 2023. "Laboratory investigations on the behavior of CBR in two expanding soils reinforced with plant fibers of varying lengths and content", Mater Today Proc, July 2023, S2214785323037884. http://doi.org/10.1016/j.matpr.2023.06.395.

[14] Gonin, H., Vandangeon, P., and Lafeuillade, M. P. 1992. "Étude sur les corrélations entre le standard et le pressiomètre penetration test", Rev Franç Géotech, 58, pp. 67–78.

[15] Idriss, I. M., and Boulanger, R. W. 2004. "Semi-empirical procedures for evaluating liquefaction potential during earthquakes", In: Proc. 11th International Conference on Soil Dynamics and Earthquake Engineering and 3rd International Conference on Earthquake Geotechnical Engineering, vol. 1, pp. 32–56. Stallion Press.

[16] Idriss, I. M. 1999. "An update to the Seed-Idriss simplified procedure for evaluating liquefaction potential", In: Proc. TRB Workshop on New Approaches to Liquefaction, Publication No. FHWA-RD-99-165, Federal Highway Administration.

[17] Ishibashi, I., and Zhang, X. 1993. "Unified dynamic shear moduli and damping ratios of sand and clay", Soil Found, 33(1), pp. 182–191.

[18] Japan National Committee on Earthquake Engineering. 1964. Niigata Earthquake of 1964, pp. S78–S109.

[19] Juang, C. H., Yuan, H., Lee, D. H., and Lin, P. S. 2003. "Simplified cone penetration test-based method for evaluating liquefaction resistance of soils", J Geotech Geoenviron Eng, 129(1), pp. 66–80.http://doi.org/10.1061/(ASCE)1090-0241(2003)129:1(66)

[20] Katsikas, C. A., and Wylie, E. B. 1982. "Sand liquefaction: inelastic effective stress model", J Geotech Eng Div, 108(1), pp. 63–81. http://doi.org/10.1061/AJGEB6.0001239

[21] Kizshida, H. 1966. "Damage to reinforced concrete buildings in Niigata city with special reference to foundation engineering", Soil Found, 6(1), pp. 71–88.

[22] Koizumi, Y. 1966. "Change in density of sand subsoil caused by the Niigata earthquake", Soil Found, 6(2), pp. 38–44.

[23] Latifi, F. E., and Baba, K. 2024. "Predicting liquefaction susceptibility in North-East Morocco: comparative analysis of semi-empirical methods and UBC3D-PLM model", Civil Eng Archit, 12(3),

pp.1474–1489.
http://doi.org/10.13189/cea.2024.120316

[24] Latifi, F. E., Baba, K., Ardouz, G., and El Bouanani, L. 2024. "Evaluation of liquefaction potential based on cone penetration test (CPT) and semi-empirical methods", Civil Eng J, 9(2).

[25] Latifi, F. E., Baba, K., Bahi, L., Touijrate, S., and Cherradi, C. 2020. "Semi-empirical method for evaluating risk of liquefaction during earthquakes: a study case of Rhiss Dam", E3S Web Conf, 150, 01004.http://doi.org/10.1051/e3sconf/202015001004

[26] Latifi, F. E., Baba, K., Bahi, L., Touijrate, S., and Cherradi, C. 2020. "Semi-empirical method for evaluating risk of liquefaction during earthquakes: a study case of Rhiss Dam", E3S Web Conf, 150, 01004.
http://doi.org/10.1051/e3sconf/202015001004

[27] Liao, S. S. C., and Whitman, R. V. 1986. "A catalog of liquefaction and non-liquefaction occurrences during earthquakes", Massachusetts Institute of Technology, Department of Civil Engineering, Cambridge, MA, 117 pp.

[28] Michard, A. 2008. "Frizon de Lamotte et al 2008 Atlas System".

[29] Mohey Mohamed, A., Abd El Fattah, M., Mohamedhassan, A., and Moussa Abu Bakr, A. 2020. "Numerical analysis of liquefaction phenomenon by using UBC3D-PLM constitutive model", J Adv Eng Trends, 38(2), pp. 81–96. http://doi.org/10.21608/jaet.2020.73029

[30] Nemati, N. S., and Shokooh, A. 1979. "Une approche unifiée à densification et liquéfaction de sable sans cohésion dans la taille cyclique", Can Geotech J, 16, pp. 659–678.

[31] Ohsaki, Y. 1969. "Niigata earthquake, 1964: Building damage and soil conditions", Soil Found, 6(2), pp. 14–37.

[32] Olsen, R. S. 1997. "Cyclic liquefaction based on the cone penetrometer test", In: Proc. NCEER Workshop on Evaluation of Liquefaction Resistance of Soils, Buffalo, NY, pp. 225–276.

[33] Petalas, A., and Galavi, V. 2013. "PLAXIS liquefaction model UBC3D-PLM".

[34] Petalas, A., and Galavi, V. 2012. "PLAXIS liquefaction model UBC3D-PLM", Delft: PLAXIS B.V.

[35] Poulos, S. J., Castro, G., and France, J. W. 1985. "Liquefaction evaluation procedure", J Geotech Eng, 111(6), pp. 772–792.

[36] Robertson, P. K., and Wride, C. E. 1998. "Evaluating cyclic liquefaction potential using the cone penetration test", Can Geotech J, 35(3), pp. 442–459. http://doi.org/10.1139/t98-017

[37] Royaume du Maroc, Ministère de l'Habitat, de l'Urbanisme et de la Politique de la Ville. 2001. The Seismic Construction Regulations, Report RPS2000, Rabat, Morocco.

[38] Seed, H. B., and Idriss, I. M. 1971. "Simplified procedure for evaluating soil liquefaction potential", J Soil Mech Found Div, ASCE, 97(SM9), pp. 1249–1273.

[39] Seed, H. B., Mori, K., and Chan, C. K. 1975. "Influence of seismic history on the liquefaction characteristics of sands", Report No. EERC 75-25, Earthquake Engineering Research Center, University of California, Berkeley.

[40] Seed, H. B., Tokimatsu, K., Harder Jr., L. F., and Chung, R. 1984. "The influence of SPT procedures on soil liquefaction resistance evaluations", Report No. UCB/EERC-84/15, Earthquake Engineering Research Center, University of California, Berkeley.

[41] Seed, H. B., and Idriss, I. M. 1971. "Simplified procedure for evaluating soil liquefaction potential", J Soil Mech Found Div, ASCE, 97(SM9), pp. 1249–1273.

[42] Seed, H. B., and Idriss, I. M. 1982. Ground Motions and Soil Liquefaction during Earthquakes, Earthquake Engineering Research Institute, University of California, Berkeley, USA.

[43] "Séisme du 28 septembre 2018 (magnitude 7,5) en Indonésie : une vitesse de propagation inhabituelle !" 2018. Echosciences-PACA.

[44] Timothy, J. W., Rodney, A. C., and Gerald, L. B. 1995. Liquefaction features from a subduction zone earthquake: Preserved examples from the 1964 Alaska Earthquake, Washington Division of Geology and Earth Resources, Report of Investigations 32.

[45] Touijrate, S., Baba, K., Ahatri, M., and Bahi, L. 2018. "The liquefaction potential of sandy silt layers using CPT tests: case study from the Casablanca–Tangier high-speed rail line (LGV) in Morocco", Int J Civ Eng Technol, 9, pp. 1644–1656.

[46] Touijrate, S., Baba, K., Ahatri, M., and Bahi, L. 2019. "The liquefaction potential of sandy silt layers using the correlation between penetrometer test and SPT test", In: Choudhury, D., El-Zahaby, K. M., and Idriss, I., eds. Dynamic Soil-Structure Interaction for Sustainable Infrastructures, in Sustainable Civil Infrastructures. Cham: Springer

InternationalPublishing,pp.8–26.
http://doi.org/10.1007/978-3-030-01920-4_2

[47] Tsegaye, A. B. 2010. "PLAXIS liquefaction model (UBC3D)", Report No. 1. Delft: PLAXIS B.V.

[48] Youd, T. L., Idriss, I. M., Andrus, R. D., Arango, I., Castro, G., and Christian, J. T. 2001. "Liquefaction resistance of soils: Summary report from the 1996 NCEER and 1998 NCEER/NSF workshop on evaluation of liquefaction resistance of soils", J Geotech Geoenviron Eng, 127(10), pp. 817–833.

[49] Youd, T. L. 2014. "Ground failure investigations following the 1964 Alaska earthquake", Proc. 10th US Natl Conf Earthq Eng, Anchorage, Alaska, USA, July 21–25, 2014